Phosphorus Monoxide Coordination Chemistry: Synthesis and Structural Characterization of Tetranuclear Clusters Containing a PO Ligand

Weibin Wang,[†] John F. Corrigan,[†] Simon Doherty,[†] Gary D. Enright,[‡] Nicholas J. Taylor,[†] and Arthur J. Carty*[,†,‡]

Guelph-Waterloo Centre for Graduate Work in Chemistry, Waterloo Campus, Department of Chemistry, University of Waterloo, Waterloo, Ontario, Canada N2L 3G1, and Steacie Institute for Molecular Sciences, National Research Council of Canada, Ottawa, Ontario, Canada K1A 0R6

Received January 18, 1996[⊗]

The clusters $Ru_4(CO)_{13}(PNPr^i_2)$ (**1**) and $Os_4(CO)_{13}(PNPr^i_2)$ (**4**) have been prepared via the reactions of $Cl_2PNPr^i_2$ with respectively $[Ru_4(CO)_{13}]^{2-}$ and the reaction product of $Na_2[Os(CO)_4]$ and $Os_3(CO)_{12}$. The successful synthesis of **4** suggests that the reaction of $Na_2[Os(CO)_4]$ with $Os_3(CO)_{12}$ generates $[Os_4(CO)_{13}]^{2-}$, thus providing a relatively easy route for the preparation of this dianion. Thermal decarbonylation of **1** and **4** affords the tetranuclear clusters $M_4(CO)_{12}(PNPr^i_2)$ (M = Ru, **2**, and Os, **5**), which upon chromatography and subsequent metathesis with $Et_4N[Cl]$ afford the $[H_2NPr^i_2]^+$ and $[Et_4N]^+$ salts of $[M_4(CO)_{12}(PO)]^-$ (M = Ru, **3**, and Os, **6**), respectively. The structures of **1**, **2**, **3**$[H_2NPr^i_2]$, **4**, and **6**$[Et_4N]$ were determined by X-ray crystallography. The M_4P frameworks in **1** and **4** form a square pyramidal arrangement with the P atom occupying a basal position. The molecular structure of **2** reveals a five-vertex polyhedron with the $PNPr^i_2$ ligand capping one face of a Ru_4 tetrahedron. The arrangement of metal and phosphorus atoms in **3**$[H_2NPr^i_2]$ and **6**$[Et_4N]$ remains similar to that in **2**. The phosphorus monoxide ligand, in each case, triply bridges a M_3 face of the tetrahedral M_4 skeleton with the P−O vector essentially perpendicular to this face. The interatomic P−O distances in **3**$[H_2NPr^i_2]$ and **6**$[Et_4N]$ suggest double-bond character for the P−O moiety. Cleavage of the PN bond of an aminophosphinidene ligand followed by P−O bond formation may have general applicability for the preparation of metal clusters containing a PO ligand.

Introduction

As the phosphorus congener of nitric oxide, the diatomic molecule PO has attracted both theoretical and spectroscopic interest.[1] Phosphorus monoxide is likely the most abundant P-containing molecule in dense interstellar clouds and has posed a challenge to astrochemists.[2] In the isolated, free state PO is a radical with a doublet $^2\Pi$r ground state and a doublet $^2\Sigma$ first excited state.[3] Further comparison with NO is sterile, however, since little is known of the chemistry of PO as a result of the inherent instability of this molecule relative to the better known oxides of phosphorus P_4O_6 and P_4O_{10}.[4] Unlike NO, which has a very well developed coordination chemistry,[5] PO has not been extensively explored as a ligand due to a lack of methods to access PO or complexes containing a coordinated PO molecule. In fact the first compound containing a PO ligand, $(\eta^5\text{-}C_5HPr^i_4)_2Ni_2W(CO)_4(PO)_2$,[6] reported by Scherer *et al.* in 1991, was prepared by the oxidation of $(\eta^5\text{-}C_5HPr^i_4)_2Ni_2W(CO)_4P_2$ with bis(trimethylsilyl) peroxide. Until our recent communication on $[Ru_4(CO)_{12}(PO)]^-$,[7] this heterometallic cluster was the only known complex containing a PO ligand.

In this paper we report a strategy for accessing coordinated PO via P−N bond cleavage of aminophosphinidene (μ_3-$PNPr^i_2$) ligands. The synthesis and characterization of $M_4(CO)_x(\mu_3\text{-}PNPr^i_2)$ (x = 13, M = Ru, **1**, and Os, **4**; x = 12, M = Ru, **2**, and Os, **5**) and $[M_4(CO)_{12}(PO)][Cat.]$ (M = Ru, **3**[Cat.], and Os, **6**[Cat.]; Cat. = $H_2NPr^i_2$, Et_4N) are described. The latter molecules represent the first series of PO complexes to be characterized.

Experimental Section

General Procedures. Syntheses were carried out using either a nitrogen-atmosphere Braun glovebox or standard Schlenk techniques. Solvents, unless otherwise stated, were dried and distilled under nitrogen prior to use. Separation of

[†] University of Waterloo.
[‡] National Research Council of Canada.
[⊗] Abstract published in *Advance ACS Abstracts,* May 1, 1996.

(1) (a) Butler, J. E.; Kawaguchi, K.; Hirota, E. *J. Mol. Spectrosc.* **1983**, *101*, 161. (b) Andrews, L.; Withnall, R. *J. Am. Chem. Soc.* **1988**, *110*, 5605. (c) Andrews, L.; McCluskey, M.; Mielke, Z.; Withnall, R. *J. Mol. Struct.* **1990**, *222*, 95. (d) Lohr, L. L. *J. Phys. Chem.* **1984**, *88*, 5569. (e) Hamilton, P. A.; Murrells, T. P. *J. Phys. Chem.* **1986**, *90*, 182.

(2) Matthews, H. E.; Feldman, P. A.; Bernath, P. F. *Astrophys. J.* **1987**, *312*, 358.

(3) *Molecular Spectra and Molecular Structure*; Herzberg, G., Ed.; D. Van Nostrand Co.: New York, 1950; Vol. 1.

(4) (a) Maxwell, L. R.; Hendricks, S. B.; Deming, L. S. *J. Chem. Phys.* **1937**, *5*, 626. (b) Hampson, G. C.; Stosick, A. J. *J. Am. Chem. Soc.* **1938**, *60*, 1814. (c) de Decker, H. C. J.; MacGillavry, C. H. *Recl. Trav. Chim.* **1941**, *60*, 153.

(5) (a) Richter-Addo, G. B.; Legzdins, P. *Metal Nitrosyls*; Oxford University Press: New York, 1992. (b) Gladfelter, W. L. *Adv. Organomet. Chem.* **1985**, *24*, 41.

(6) Scherer, O. J.; Braun, J.; Walther, P.; Heckmann, G.; Wolmershauser, G. *Angew. Chem., Int. Ed. Engl.* **1991**, *30*, 852.

(7) Corrigan, J. F.; Doherty, S.; Taylor, N. J.; Carty, A. J. *J. Am. Chem. Soc.* **1994**, *116*, 9799.

S0276-7333(96)00032-5 CCC: $12.00

products was accomplished by column chromatography and TLC using oven-dried (150 °C, over 48 h) silica gel (70−230 mesh). Infrared spectra were recorded on a Nicolet 520 FTIR spectrometer. NMR spectra were recorded on Bruker AC-200 and AM-250 instruments at field strengths of 81.02 and 101.27 MHz, respectively, for $^{31}P\{^1H\}$ and 50.32 and 62.97 MHz, respectively, for $^{13}C\{^1H\}$. Microanalyses were carried out by M-H-W Laboratories, Phoenix, AZ. All chemicals were commercially supplied and used without further purification. The osmium salt $Na_2[Os(CO)_4]$ was prepared by the literature method,[8] and $K_2[Ru_4(CO)_{13}]$ was synthesized via a modification of the literature procedure (see the preparation of **1**).[9]

Preparation of $Ru_4(CO)_{13}(PNPr^i_2)$ (1). To a mixture of $Ru_3(CO)_{12}$ (~1 g), benzophenone, and potassium (molar ratio 1/1.5/1.5) was added THF (20 mL) dropwise over a 2 h period. The solution was stirred vigorously for 24 h yielding a deep red solution of $K_2[Ru_4(CO)_{13}]$. This was followed by the dropwise addition of 0.75 equiv (to $Ru_3(CO)_{12}$) of $Cl_2PNPr^i_2$. After the solution was stirred for a further 2 h, the solvent was removed in vacuo to give a red solid which was dissolved in CH_2Cl_2 and absorbed onto dried silica gel. Removal of CH_2Cl_2 and column chromatography with hexane as the eluant led to isolation of the desired product. Air-stable, dark red crystals of **1** (0.19−0.23 g, 18−22%) were obtained from the recrystallization from CH_2Cl_2/MeOH at −10 °C. IR (CH_2Cl_2): ν(CO) 2092 w, 2053 vs, 2047 s, 2034 m, 2002 m, 1979 w cm^{-1}. ^1H NMR ($CDCl_3$): δ 4.32 (dsept, $^3J_{PH}$ = 11.9 Hz, $^3J_{HH}$ = 6.9 Hz, CH), 1.50 (d, $^3J_{HH}$ = 6.9 Hz, CH_3). $^{31}P\{^1H\}$ NMR ($CDCl_3$): δ 466.0(s). $^{13}C\{^1H\}$ NMR ($CDCl_3$): δ 199.7 (br s, CO), 195.6 (br s, CO), 192.0 (br s, CO), 56.2 (d, $^2J_{PC}$ = 5.5 Hz, CH), 23.5 (d, $^3J_{PC}$ = 3.0 Hz, CH_3). Anal. Calcd for $C_{19}H_{14}NO_{13}PRu_4$: C, 25.37; H, 1.57. Found: C, 25.10; H, 1.80.

Preparation of $Ru_4(CO)_{12}(PNPr^i_2)$ (2). A solution of **1** (103 mg, 0.115 mmol) in hexane was brought to reflux for 3 h during which a color change from red/purple to brown/orange occurred. After removal of the solvent the resulting oily residue was dissolved in CH_2Cl_2 and absorbed onto TLC plates. Elution with CH_2Cl_2/hexane (10/90) under a nitrogen atmosphere afforded traces of **1** and a second, major orange band from which dark red crystals of **2** (64 mg, 64%) were obtained from toluene at −10 °C. IR (CH_2Cl_2): ν(CO) 2086 w, 2034 vs, 2007 w, 1990 w cm^{-1}. ^1H NMR ($CDCl_3$): δ 4.42 (dsept, $^3J_{PH}$ = 15.3 Hz, $^3J_{HH}$ = 6.8 Hz, CH), 1.62 (d, $^3J_{HH}$ = 6.8 Hz, CH_3). $^{31}P\{^1H\}$ NMR ($CDCl_3$): δ 467.0 (s). $^{13}C\{^1H\}$ NMR ($CDCl_3$): δ 199.0 (br s, CO), 55.5 (s, CH), 23.4 (d, $^3J_{PC}$ = 3.0 Hz, CH_3). Anal. Calcd for $C_{18}H_{14}NO_{12}PRu_4$: C, 24.80; H, 1.62. Found: C, 24.56; H, 1.63.

Preparation of $[Ru_4(CO)_{12}(PO)][Cat.]$ (3[Cat.], Cat. = $H_2NPr^i_2$, Et_4N). A sample of **2** (50 mg, 0.057 mmol) was dissolved in a minimum amount of CH_2Cl_2 and absorbed onto an activated TLC plate. The product was allowed to slowly elute under nitrogen for 3 h with nondried solvents (CH_2Cl_2/hexane, 10/90). A front-running dark orange band was followed closely by one which was streaky and pale orange in color. The two fractions were collected together. Extraction using CH_2Cl_2 led to the recovery of 19 mg of **2**. A second extraction sequence using CH_3CN gave 26 mg (51%) of red crystalline **3**[$H_2NPr^i_2$] upon recrystallization from CH_2Cl_2/C_7H_8. The reaction of a slight excess of Et_4NCl with **3**[$H_2NPr^i_2$] produced **3**[Et_4N] in quantitative yield, as monitored by IR spectroscopy, and pure samples of **3**[Et_4N] were obtained by crystallization from CH_2Cl_2/hexane. Compound **3**[$H_2NPr^i_2$]: IR (CH_2Cl_2) ν(CO) 2075 w, 2024 vs, 1978 w, ν(PO) (KBr) 1075 cm^{-1}; ^1H NMR (CD_2Cl_2) δ 7.32 (br s, NH_2), 3.48 (sept, $^3J_{HH}$ = 6.4 Hz, CH), 1.41 (d, $^3J_{HH}$ = 6.2 Hz, CH_3); $^{31}P\{^1H\}$ NMR (CD_2Cl_2) δ 476.2 (s). Anal. Calcd for $C_{18}H_{16}NO_{13}PRu_4$: C, 24.30, H, 1.81. Found: C, 24.42; H, 1.53. Compound **3**[Et_4N]: IR (CH_2Cl_2) ν(CO) 2072 w, 2019 vs, 1974 w, ν(PO) (KBr) 1169 cm^{-1}; ^1H NMR (CD_2Cl_2) δ 3.27 (q, $^3J_{HH}$ = 7.3 Hz, CH_2), 1.35 (tt, $^3J_{HH}$ = 7.3 Hz, $^5J_{HH}$ = 1.7 Hz, CH_3); $^{31}P\{^1H\}$ NMR (CD_3CN) δ 474.2 (s). Anal. Calcd for $C_{20}H_{20}NO_{13}PRu_4$: C, 26.18; H, 2.20. Found: C, 26.36, H, 2.40.

Preparation of $Os_4(CO)_{13}(PNPr^i_2)$ (4). A solution of $Na_2[Os(CO)_4]$ (152 mg, 0.437 mmol) and $Os_3(CO)_{12}$ (376 mg, 0.415 mmol) in THF (50 mL) was stirred in the dark for 4 days. After dropwise addition of $Cl_2NPr^i_2$ (89 mg, 0.44 mmol), stirring was continued for 2 h. The products were isolated using TLC plates with CH_2Cl_2/hexane (10/90) as the eluant. Extraction of the orange band with CH_2Cl_2 afforded, after removal of solvent, 171 mg (33%) of **4** which yielded red crystals from hexane on refrigeration. IR (CH_2Cl_2): ν(CO) 2099 w, 2052 br, vs, 2037 m, 2000 m cm^{-1}. ^1H NMR ($CDCl_3$): δ 3.91 (sept, $^3J_{HH}$ = 6.8 Hz, CH), 1.50 (d, $^3J_{HH}$ = 6.9 Hz, CH_3). $^{31}P\{^1H\}$ NMR ($CDCl_3$): δ 253.4 (s). Anal. Calcd for $C_{19}H_{14}NO_{13}POs_4$: C, 18.17; H, 1.12. Found: C, 18.23; H, 1.09.

Preparation of $Os_4(CO)_{12}(PNPr^i_2)$ (5). The thermolysis of **4** was carried out in a manner similar to that used to prepare **2** except that refluxing toluene and a reaction period of 12 h were employed. The isolation of **5** was similar to that of **2**. A pure sample of **5** (65% in yield) was obtained after washing the solid with small aliquots of hexane. IR (CH_2Cl_2): ν(CO) 2089 w, 2038 vs, 2003 w, 1987 w cm^{-1}. ^1H NMR ($CDCl_3$): δ 4.49 (dsept, $^3J_{PH}$ = 17.9 Hz, $^3J_{HH}$ = 6.8 Hz, CH), 1.65 (d, $^3J_{HH}$ = 6.8 Hz, CH_3). $^{31}P\{^1H\}$ NMR ($CDCl_3$): δ 378.8 (s). $^{13}C\{^1H\}$ NMR ($CDCl_3$): δ 176.6 (s, CO), 174.5 (d, $^2J_{PC}$ = 12.4 Hz, CO), 55.2 (d, $^2J_{PC}$ = 2.8 Hz, CH), 22.5 (d, $^3J_{PC}$ = 3.9 Hz, CH_3). Anal. Calcd for $C_{18}H_{14}NO_{12}POs_4$: C, 17.60; H, 1.15. Found: C, 17.79; H, 1.13.

Preparation of $[Os_4(CO)_{12}(PO)][Cat.]$ (6[Cat.]; Cat. = $H_2NPr^i_2$, Et_4N). Compound **6**[$H_2NPr^i_2$] was synthesized in similar fashion to the Ru analogue **3**[$H_2NPr^i_2$] except that the elution was conducted for over 6−9 h. Recrystallization from CH_2Cl_2/hexane gave light amber crystals of **6**[$H_2NPr^i_2$] (34−38% in yield). The reaction of a slight excess of Et_4NCl with **6**[$H_2NPr^i_2$] in CH_2Cl_2 afforded **6**[Et_4N] in quantitative yield, and pure samples of **6**[Et_4N] were obtained by crystallization from CH_2Cl_2/hexane. Compound **6**[$H_2NPr^i_2$]: IR (CH_2Cl_2) ν(CO) 2080 w, 2032 vs, 2021 sh, 1979 w, ν(PO) (Nujol) 1156 cm^{-1}; ^1H NMR ($CDCl_3$) δ 7.49 (br s, NH_2), 3.61 (sept, $^3J_{HH}$ = 6.4 Hz, CH), 1.56 (d, $^3J_{HH}$ = 6.6 Hz, CH_3); $^{31}P\{^1H\}$ NMR ($CDCl_3$) δ 410.9 (s). Anal. Calcd for $C_{18}H_{16}NO_{13}POs_4$: C, 17.35; H, 0.73. Found: C, 17.54; H, 0.80. Compound **6**[Et_4N]: IR (CH_2Cl_2) ν(CO) 2077 w, 2027 vs, 2016 sh, 1974 w, ν(PO) (Nujol) 1176 cm^{-1}; ^1H NMR ($CDCl_3$) δ 3.38 (q, $^3J_{HH}$ = 7.2 Hz, CH_2), 1.42 (br t, $^3J_{HH}$ = 6.5 Hz, CH_3); $^{31}P\{^1H\}$ NMR ($CDCl_3$) δ 403.8 (s). Anal. Calcd for $C_{20}H_{20}NO_{13}POs_4$: C, 18.85; H, 1.58. Found: C, 19.02; H, 1.63.

X-ray Analyses. Single crystals of each compound were obtained by recrystallization: from CH_2Cl_2/MeOH for **1**, toluene for **2**, CH_2Cl_2/toluene for **3**[$H_2NPr^i_2$], hexane for **4**, and CH_2Cl_2/hexane for **6**[Et_4N]. A suitable crystal of each of **1**, **2**, and **3**[$H_2NPr^i_2$] was mounted on an LT-2-equipped Siemens R3m/V diffractometer, and the intensity data were collected with the use of graphite-monochromated Mo Kα radiation. Intensity data for the osmium clusters were collected on an Enraf-Nonius CAD-4F diffractometer, using graphite-monochromated Cu radiation. Background measurements were made by extending the scan width by 25% on each side of the scan for the ruthenium compounds or by taking a stationary background count at each end of the scan (for $^1/_{10}$ the scan time) combined with the profile analysis[10] for the osmium compounds. Two intensity standards, monitored every 100 reflections during the data collection, showed no significant changes except for **6**[Et_4N] in which case they decreased by 12−15%. Unit cell parameters were determined from 25 (for

(8) (a) Carter, W. J.; Kelland, J. W.; Okrasinski, S. J.; Warner, K. E.; Norton, J. R. *Inorg. Chem.* **1982**, *21*, 3955. (b) Collman, J. P.; Murphy, D. W.; Fleischer, E. B.; Swift, D. *Inorg. Chem.* **1974**, *13*, 1.

(9) Bhattacharyya, A. A.; Nagel, C. C.; Shore, S. G. *Organometallics* **1983**, *2*, 1187.

(10) (a) Gabe, E. J.; LePage, Y.; Charland, J.-P.; Lee, F. L.; White, P. S. *J. Appl. Crystallogr.* **1989**, *22*, 384. (b) Grant, D. F.; Gabe, E. J. *J. Appl. Crystallogr.* **1978**, *11*, 114.

Table 1. Summary of Crystal Data and Details of Intensity Collection for 1, 2, 3[$H_2NPr^i_2$], 4, and 6[Et_4N]

	compound		
	1	2	**3**[$H_2NPr^i_2$]
molecular formula	$C_{19}H_{14}NO_{13}PRu_4$	$C_{18}H_{14}NO_{12}PRu_4$	$C_{18}H_{16}NO_{13}PRu_4$
fw	899.6	871.6	889.6
temp (K)	200	200	295
cryst syst	orthorhombic	triclinic	triclinic
space group	Pbca	$P\bar{1}$	$P\bar{1}$
a, Å	14.666(5)	8.656(1)	8.983(2)
b, Å	13.385(5)	11.509(2)	11.514(2)
c, Å	27.710(8)	13.760(5)	14.030(2)
α, deg		89.84(2)	80.89(2)
β, deg		89.45(1)	87.00(2)
γ, deg		68.47(1)	77.00(2)
V, Å^3	5439(3)	1275.2(4)	1395.8(3)
Z	8	2	2
D_{calc}, g cm^{-3}	2.197	2.270	2.117
μ(Mo Kα), cm^{-1}	23.00	24.46	22.39
cryst size, mm	0.21 {001} × 0.42 {221} × 0.21 {111} × 0.21 {111}	0.18 {010} × 0.40 {001} × 0.54 {110}	0.24 {100} × 0.30 {010} × 0.30 {110} × 0.068 {001}
transm coeff range[a]	0.595−0.667	0.388−0.663	0.566−0.861
scan method	*ω*	*ω*	*ω*
scan width (*ω*), deg	1.20	1.20	1.20
scan rate (*ω*), deg min^{-1}	2.93−29.30	2.93−29.30	2.93−29.30
scan range (2*θ*), deg	4−56	4−52	4−52
no. of unique rflns	6611	5034	5514
no. of obsd rflns[b]	5177	4811	4544
no. of variables	358	340	351
R[c]	0.027	0.020	0.025
R_w[d]	0.032	0.029	0.030
GOF[e]	1.91	3.58	1.84

	compound	
	4	**6**[Et_4N]
molecular formula	$C_{19}H_{14}NO_{13}POs_4$	$C_{20}H_{20}NO_{13}POs_4$
fw	1256.1	1274.1
temp (K)	295	295
cryst syst	orthorhombic	monoclinic
space group	*Pbca*	$P2_1/n$
a, Å	14.891(2)	9.207(1)
b, Å	13.446(2)	12.515(1)
c, Å	27.881(3)	25.739(2)
β, deg		95.32(1)
V, Å^3	5582(1)	2953.0(4)
Z	8	4
D_{calc}, g cm^{-3}	2.989	2.866
μ(Cu Kα), cm^{-1}	346.5	327.6
cryst size, mm	0.058 {001} × 0.060 {10$\bar{1}$} × 0.34 {110} × 0.38 {1$\bar{1}$2}	0.053 {001} × 0.073 {$\bar{2}$01} × 0.10 {2$\bar{1}$1} × 0.12 {112}
transm coeff range[a]	0.00564−0.244	0.0305−0.282
scan method	*ω*−2*θ*	*ω*−2*θ*
scan width (*ω*), deg	1.1 + 0.15 tan *θ*	1.0 + 0.15 tan *θ*
scan rate (*ω*), deg min^{-1}	2.0	2.0
scan range (2*θ*), deg	4−140	4−140
no. of unique rflns	5310	5583
no. of obsd rflns[f]	4616	4125
no. of variables	344	353
R[c]	0.036	0.045
R_w[g]	0.052	0.060
k[g]	0.0004	0.0005
GOF[e]	1.9	1.9
extinction (*g*)	1.54(8)	0.39(4)

[a] Absorption corrections. [b] $F_o > 6\sigma(F_o)$. [c] $R = \sum||F_o| - |F_c||/\sum|F_o|$. [d] $R_w = (\sum w(|F_o| - |F_c|)^2/\sum w|F_o|^2)^{1/2}$, $w = [\ \sigma^2(F_o)\ ]^{-1}$. [e] GOF = $(\sum w(|F_o| - |F_c|)^2/(\text{no. of rflns} - \text{no. of variables}))^{1/2}$. [f] $I_o > 2.5\sigma(I_o)$. [g] $R_w = (\sum w(|F_o| - |F_c|)^2/\sum w|F_o|^2)^{1/2}$, $w = [\ \sigma^2(F_o) + k(F_o)^2\ ]^{-1}$.

the Ru clusters), 24 (for **4**), and 35 (for **6**[Et_4N]) reflections widely distributed in reciprocal space. Absorption corrections were applied to the intensity data using the face-indexed numerical method.

The positions of the metal atoms were determined by Patterson syntheses (for the Ru clusters) and direct methods (for the Os clusters). Subsequent electron density difference maps revealed the remaining non-hydrogen atoms. All non-hydrogen atoms were assigned anisotropic thermal parameters. Hydrogen atoms were placed in calculated positions. Complex scattering factors[11] for neutral atoms were used in the calculation of structure factors. An extinction parameter was introduced for the refinement of **4** and **6**[Et_4N]. All computations were carried out on Micro Vax II and Vax 3000 computers and Silicon Graphics Indigo Work Stations using SHELXTL PLUS software and the NRCVAX[10a] crystal structure system. Crystallographic data are summarized in Table 1. Atomic coordinates for **1**, **2**, **3**[$H_2NPr^i_2$], **4**, and **6**[Et_4N] are

(11) (a) *International Tables for X-ray Crystallography*; Kynoch Press: Birmingham, England, 1974; Vol. IV, p 99. (b) Stewart, R. F.; Davidson, E. R.; Simpson, W. T. *J. Chem. Phys.* **1965**, *42*, 3175.

Table 2. Selected Bond Lengths (Å) and Angles (deg) for 1 and 4

	1	4
	Bond Lengths	
M(1)−M(2)	2.798(1)	2.793(1)
M(1)−M(3)	2.856(1)	2.912(1)
M(2)−M(3)	2.960(1)	2.991(1)
M(2)−M(4)	2.775(1)	2.805(1)
M(3)−M(4)	2.883(1)	2.894(1)
M(1)−P(1)	2.323(1)	2.337(3)
M(2)−P(1)	2.413(1)	2.446(3)
M(4)−P(1)	2.310(1)	2.341(3)
P(1)−N(1)	1.671(4)	1.685(8)
	Bond Angles	
M(3)−M(1)−P(1)	75.7(1)	75.9(1)
M(1)−M(3)−M(4)	88.3(1)	87.7(1)
M(3)−M(4)−P(1)	75.4(1)	76.2(1)
M(1)−P(1)−M(4)	119.3(1)	118.7(1)
M(3)−C(7)−O(7)	166.3(4)	171.7(10)
M(3)−C(8)−O(8)	170.3(4)	172.5(10)
M(3)−C(9)−O(9)	176.7(4)	175.5(11)
M(3)−C(10)−O(10)	174.2(4)	174.3(11)

Table 3. Selected Bond Lengths (Å) and Angles (deg) for 2

	Bond Lengths		
Ru(1)−Ru(2)	2.848(1)	Ru(3)−Ru(4)	2.890(1)
Ru(1)−Ru(3)	2.787(1)	Ru(2)−P(1)	2.270(1)
Ru(1)−Ru(4)	2.810(1)	Ru(3)−P(1)	2.298(1)
Ru(2)−Ru(3)	2.858(1)	Ru(4)−P(1)	2.309(1)
Ru(2)−Ru(4)	2.847(1)	P(1)−N(1)	1.636(3)
	Bond Angles		
Ru(2)−C(4)−O(4)	162.7(3)	Ru(3)−C(8)−O(8)	174.9(5)
Ru(2)−C(6)−O(6)	177.4(4)	Ru(4)−C(11)−O(11)	176.0(4)
Ru(3)−C(7)−O(7)	167.5(4)	Ru(4)−C(12)−O(12)	174.0(3)

Table 4. Selected Bond Lengths (Å) and Angles (deg) for 3[$H_2NPr^i_2$] and 6[Et_4N]

	3[$H_2NPr^i_2$]	**6**[Et_4N]
	Bond Lengths	
M(1)−M(2)	2.799(1)	2.824(1)
M(1)−M(3)	2.788(1)	2.811(1)
M(1)−M(4)	2.818(1)	2.826(1)
M(2)−M(3)	2.865(1)	2.882(1)
M(2)−M(4)	2.856(1)	2.883(1)
M(3)−M(4)	2.855(1)	2.879(1)
M(2)−P(1)	2.297(1)	2.314(4)
M(3)−P(1)	2.282(1)	2.294(4)
M(4)−P(1)	2.293(1)	2.321(3)
P(1)−O(13)	1.509(3)	1.476(10)
	Bond Angles	
M(2)−C(4)−O(4)	172.3(4)	178.2(15)
M(2)−C(6)−O(6)	179.0(4)	177.9(13)
Ru(3)−C(7)−O(7)	167.6(5)	175.5(14)[a]
Ru(3)−C(8)−O(8)	176.3(4)	174.6(22)[b]
M(4)−C(11)−O(11)	171.1(5)	173.6(19)
M(4)−C(12)−O(12)	177.8(6)	179.0(14)

[a] The corresponding angle is Os(3)−C(9)−O(9). [b] The corresponding angle is Os(3)−C(7)−O(7).

given in the Supporting Information. Selected bond lengths and angles for **1**, **2**, **3**[$H_2NPr^i_2$], **4**, and **6**[Et_4N] are tabulated in Tables 2−4, respectively.

Results and Discussion

Synthesis of $M_4(CO)_{13}(PNPr^i_2)$ (M = Ru, 1, and Os, 4). The synthetic route to **1** and **4** is described in eq 1. This reaction, which has previously been used to

$$[M_4(CO)_{13}]^{2-} + Cl_2PNPr^i_2 \rightarrow M_4(CO)_{13}(\mu_3\text{-}PNPr^i_2) \quad (1)$$

synthesize $Ru_4(CO)_{13}(\mu_3$-PPh), provides **1** in approximately 20% yields and represents a viable method for tailoring the electronic and steric properties of the phosphinidene ligands in these clusters.

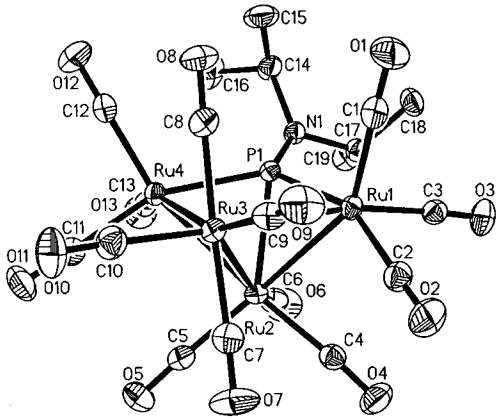

Figure 1. Molecular structure of $Ru_4(CO)_{13}(PNPr^i_2)$ (**1**).

The tetraosmium anion $[Os_4(CO)_{13}]^{2-}$ has been described by Shore and co-workers[12] as the product of the reaction of $[Os_3(CO)_{11}]^{2-}$ with $Os(CO)_5$, the latter being generated via the oxidation of $[Os(CO)_4]^{2-}$ by CO_2.[12] In our hands this procedure generated a red solution which, upon treatment with $Cl_2PNPr^i_2$, led to the isolation of **4** in very low yield. Another route to **4** was therefore sought.

The reaction of $Na_2[Os(CO)_4]$ with $Os_3(CO)_{12}$ in THF (molar ratio 1:1) gave a first pink and then red solution over a period of 30 min. Monitoring the reaction (for 4 days) by IR spectroscopy showed a decrease of intensities of ν(CO) bands at 2038 m, 1972 s, 1952 vs, and 1889 m cm^{-1} (a pattern similar to that of $K_2[Os_3(CO)_{11}]$[12]) and an increase of intensity for a very strong band at 1989 cm^{-1} likely due to $Na_2[Os_4(CO)_{13}]$.[9] These observations suggest the initial formation of $[Os_3(CO)_{11}]^{2-}$ followed by conversion to $[Os_4(CO)_{13}]^{2-}$. No conclusive IR evidence for the formation of $Os(CO)_5$ was found, but bands of $Os(CO)_5$ could be obscured by the ν(CO) bands of the cluster anions. Addition of $Cl_2PNPr^i_2$ to the red solution afforded **4** in 33% yield after chromatography. The reaction scheme is shown in eq 2. The successful synthesis of **4** clearly shows a viable route to the preparation of $[Os_4(CO)_{13}]^{2-}$.

$$\begin{array}{l} Na_2[Os(CO)_4] + Os_3(CO)_{12} \longrightarrow Na_2[Os_3(CO)_{11}] + \{Os(CO)_5\} \\ \qquad\qquad\qquad\qquad\qquad\qquad\qquad\qquad \text{dark} \downarrow \text{4 days, R. T.} \\ Os_4(CO)_{13}(\mu_3\text{-}PNPr^i_2) \xleftarrow{Cl_2PNPr^i_2} Na_2[Os_4(CO)_{13}] \\ \quad \mathbf{4} \end{array} \quad (2)$$

Spectroscopic and Structural Characterization. In order to determine the precise structural features of the phosphinidene clusters **1** and **4** single-crystal X-ray analyses were carried out. The structures of the two molecules are composed in Figures 1 and 2 and consist of a distorted *nido* square pyramidal M_4P stereochemistry with the phosphorus atom occupying a vertex of the base of the pyramid. There is a very close resemblance to the isoelectronic $M_4(CO)_{13}(\mu_3$-PPh) (M = Ru,

(12) Krause, J. A.; Siriwardane, U.; Salupo, T. A.; Wermer, J. R.; Knoeppel, D. W.; Shore, S. G. *J. Organomet. Chem.* **1993**, *454*, 263.

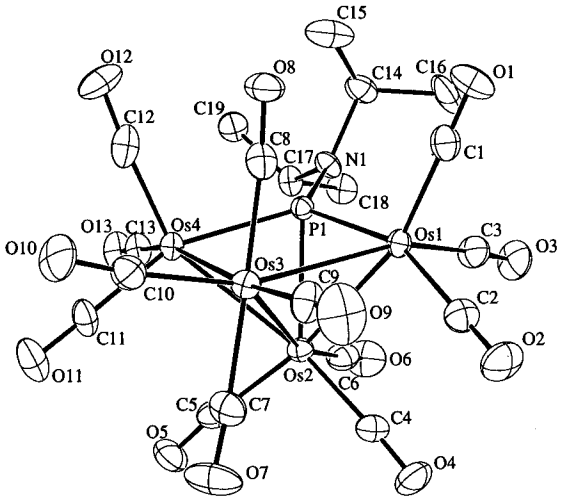

Figure 2. Molecular structure of $Os_4(CO)_{13}(PNPr^i_2)$ (**4**).

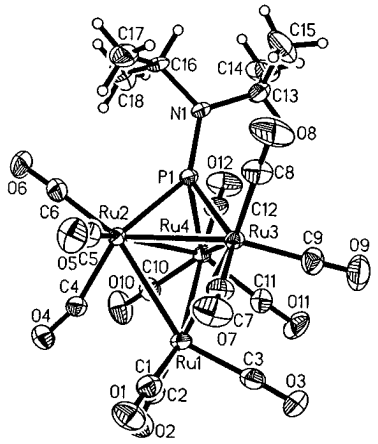

Figure 3. Molecular structure of $Ru_4(CO)_{12}(PNPr^i_2)$ (**2**).

Os).[13] In all four molecules there is a basal $M(CO)_4$ fragment occupying a hinge position in the M_4 butterfly skeleton with a μ_3-PR group diagonally opposed within the M_3P base. The orientation of the substituents on the phosphinidene ligands is such that there is a variation in dihedral angle of only 45.6−49.4° between the M_3P planes and the planes of the phosphinidene ligands (P(1)−XY_2) (X = N, Y = C in **1**, **4**; X = C, Y = C in $M_4(CO)_{13}(\mu_3$-PPh)). An interesting point about these butterfly clusters, in which a μ_3-PR ligand caps an open triangular face (M(1)−M(2)−M(4)), is that one hinge atom M(3) has four carbonyl ligands. Usually a butterfly configuration of four metal atoms is preferred only when both hinge atoms possess three ligands.[14] In the present case the M_4 skeleton is constrained to the butterfly geometry by the wing tip to wing tip interaction with the μ_3-PR group.

The metal−metal bonds involving M(3) in these isoelectronic clusters are significantly longer than the remaining M−M interactions. This partially reflects the higher coordination number (7) of M(3) but also is due to the crowded environment around M(3) demonstrated by the deviation from linearity of the M(3)−C−O angles (M(3)−C−O angles are 171.9° in **1** and 173.5° in **4**) and the interligand repulsions with neighboring CO groups on other metals. The M(1)−M(4) distances in **1** and **4** are greater than 3.5 Å, and the P(1)−M(3) separations are greater than 3.2 Å. These values preclude any significant bonding interactions.

Substitution of a μ_3-PPh group in $Ru_4(CO)_{13}(\mu_3$-PPh) and $Os_4(CO)_{13}(\mu_3$-PPh)[13] by $PNPr^i_2$ in **1** and **4** results in an overall lengthening of the metal−phosphorus bonds (Δ_{Ru-P} = 0.020 Å in **1** *vs* $Ru_4(CO)_{13}(\mu_3$-PPh); Δ_{Os-P} = 0.023 Å in **4** *vs* $Os_4(CO)_{13}(\mu_3$-PPh)). A similar Ru−P bond elongation has been noted in comparing the phosphido-bridged complexes $Ru_4(CO)_{13}(\mu_2$-$PPh_2)_2$ and $[Ru_4(CO)_{13}[\mu_2$-$P(NPr^i_2)_2]_2$ and attributed to the better π-donating ability of a diisopropylamino group to phosphorus than a phenyl group, resulting in stronger P−N but weaker P−Ru interactions.[15]

$M_4(CO)_{12}(PNPr^i_2)$ (M = Ru, 2, and Os, 5). Thermolysis of **1** and **4** at different temperatures effects their decarbonylation to afford $Ru_4(CO)_{12}(PNPr^i_2)$ (**2**) and $Os_4(CO)_{12}(PNPr^i_2)$ (**5**), respectively, in good yields. The molecular structure of **2** (Figure 3) reveals a *closo* 5-vertex M_4P polyhedron with the phosphinidene ligand capping one face of the Ru_4 tetrahedron. This is dramatically different from the structure of the isoelectronic cluster, $Fe_4(CO)_{12}(\mu_4$-$PPr^i)$,[16] in which the μ_4-PPr^i fragment lies in the equatorial plane and caps a butterfly array of metal atoms. The M_4P polyhedron in **2**, however, resembles those in $Os_4(CO)_{12}(\mu_3$-S)[17a] and $Cp^*WRu_3(CO)_{10}(\mu_3$-H)(μ_3-PPh).[17b] A similar structural arrangement is predicted for the osmium analogue **5** on the basis of the synthetic route to **5** and the similarity of the IR spectrum to that of **2**. The simple conversion of *nido*-square pyramidal **1** and **4** to *closo*-trigonal bipyramidal **2** and **5** via a loss of a 2e donor has no precedent in iron group phosphinidene chemistry.

The Ru−Ru bond lengths (Table 3) in **2** lie within the range 2.787(1)−2.890(1) Å, with the Ru(1)−Ru(2) bond spanned by a weak semibridging carbonyl ligand (Ru(1)···C(4) = 2.626(5) Å). The longest bond, between Ru(3) and Ru(4), is likely caused by the interaction of an isopropyl group with CO(8) and CO(12), as suggested from the view of Figure 3 and by the larger deviations of the Ru(3)−C(8)−O(8) and Ru(4)−C(12)−O(12) angles from 180°. The average P−Ru distance is significantly shortened on going from **1** (2.349 Å) to **2** (2.292 Å) as is the P−N distance (average 1.671(4) Å in **1**; 1.636(3) Å in **2**). The $^{13}C\{^1H\}$ spectrum of **2** at room temperature shows only a broadened signal in the carbonyl region. This indicates that the carbonyls in **2** are fluxional at room temperature on the NMR time scale. The carbonyls in **5**, however, exhibit partial rigidity. The $^{13}C\{^1H\}$ spectrum of **5** at room temperature gave a singlet at 176.6 and a doublet at 174.5 ppm with a ratio close to 1:3. It is believed that the singlet at 176.6 ppm is attributed to the three carbonyls on the apical metal atom, while the doublet at 174.5 ppm arises from a two-

(13) (a) MacLaughlin, S. A.; Carty, A. J.; Taylor, N. J. *Can. J. Chem.* **1982**, *60*, 87. (b) Cherkas, A. A.; Corrigan, J. F.; Doherty, S.; MacLaughlin, S. A.; van Gastel, F.; Taylor, N. J.; Carty, A. J. *Inorg. Chem.* **1993**, *32*, 1662.

(14) (a) Fischer, J.; Mitschler, A.; Weiss, R.; Dehand, J.; Nennig, J. F. *J. Organomet. Chem.* **1975**, *91*, C37. (b) Bhaduri, S.; Sharma, K. R.; Clegg, W.; Sheldrick, G. M.; Stalke, D. *J. Chem. Soc., Dalton Trans.* **1984**, 2851. (c) Martin, L. R.; Einstein, F. W. B.; Pomeroy, R. K. *Inorg. Chem.* **1988**, *27*, 2986. (d) Wang, W.; Davis, H. B.; Einstein, F. W. B.; Pomeroy, R. K. *Organometallics* **1994**, *13*, 5113.

(15) Corrigan, J. F.; Sun, Y.; Carty, A. J. *New. J. Chem.* **1994**, *18*, 77.

(16) Buchholz, D.; Huttner, G.; Imhof, W.; Orama, O. *J. Organomet. Chem.* **1990**, *388*, 321.

(17) (a) Adams, R. D.; Foust, D. F.; Mathur, P. *Organometallics* **1983**, *2*, 990. (b) Lin, R.-C.; Chi, Y.; Peng, S.-M.; Lee, G.-H. *Inorg. Chem.* **1992**, *31*, 3818.

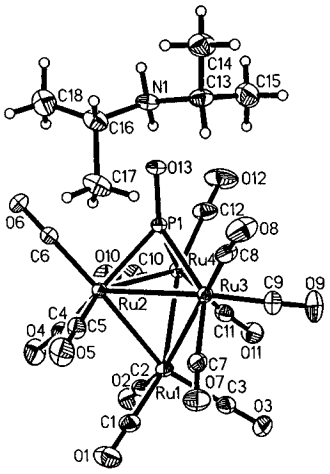

Figure 4. Molecular structure of $[Ru_4(CO)_{12}(PO)][H_2NPr^i_2]$ (**3**$[H_2NPr^i_2]$).

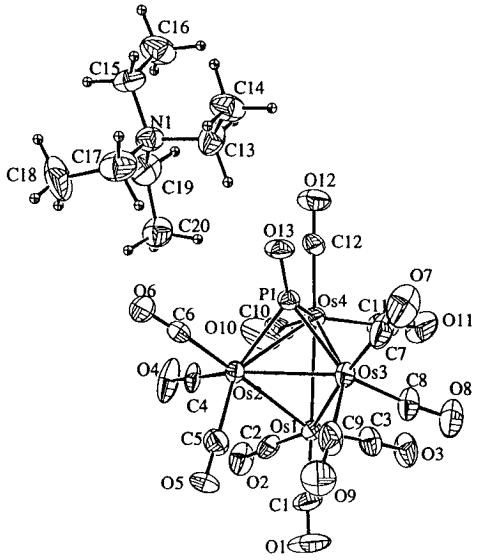

Figure 5. Molecular structure of $[Os_4(CO)_{12}(PO)][Et_4N]$ (**6**$[Et_4N]$).

bond coupling to phosphorus from the nine CO ligands in the equatorial metal sites. The fact that there exists a semibridging carbonyl on the apical ruthenium atom (Ru(1)) and one (Ru(2)) of the equatorial metal atoms is consistent with the fluxionality of **2**.[18]

$[M_4(CO)_{12}(PO)][H_2NPr^i_2]$ (M = Ru, 3$[H_2NPr^i_2]$, and Os, 6$[H_2NPr^i_2]$) and $[M_4(CO)_{12}(PO)][Et_4N]$ (M = Ru, 3$[Et_4N]$, and Os, 6$[Et_4N]$). After absorption of **2** and **5** onto silica gel, extraction with CH_2Cl_2 and CH_3CN led to the recovery of starting materials (38% for **2** and 55% for **5**) and the primary products **3**$[H_2NPr^i_2]$ and **6**$[H_2NPr^i_2]$ in 51% and 34−38% yields, respectively. Metathesis of **3**$[H_2NPr^i_2]$ and **6**$[H_2NPr^i_2]$ with Et_4NCl gave their $[Et_4N]^+$ salts.

The structures of **3**$[H_2NPr^i_2]$ (Figure 4) and **6**$[Et_4N]$ (Figure 5) consist of a tetrahedron of metal atoms capped symmetrically on one face by a PO ligand. The overall trigonal bipyramidal geometries of the Ru_4P and Os_4P polyhedra closely resemble those of the phosphinidene-capped cluster **2**. In fact the average Ru−Ru bond length in **2** (2.840 Å) is only slightly longer than in **3**$[H_2NPr^i_2]$ (2.830 Å) and the average Ru−P distances in **2** (2.292 Å) and **3**$[H_2NPr^i_2]$ (2.291 Å) are essentially identical. There are no semibridging CO groups in **3**$[H_2NPr^i_2]$ and **6**$[Et_4N]$, with the closest contact between a metal atom and a nonbonded carbon atom being 2.79(1) and 2.95(1) Å, respectively.

The major structural features of **3**$[H_2NPr^i_2]$ and **6**$[Et_4N]$ are the coordinated phosphorus monoxide ligand. The P−O bond lengths in **3**$[H_2NPr^i_2]$ and **6**$[Et_4N]$ are 1.509(3) and 1.476(10) Å. These distances are in good agreement with reported values of 1.46−1.48 Å calculated from spectroscopic parameters[1a,d] for the free PO molecule and correspond with a value of 1.48 Å found in the only other PO cluster characterized to date namely $(\eta^5\text{-}C_5HPr^i_4)_2Ni_2W(CO)_4(PO)_2$.[6] Further evidence that the P−O bond in the Ru_4 and Os_4 clusters has multiple-bond character can be seen from a comparison of P−O distances with values in tertiary phosphine oxides such as Ph_3PO (1.48 Å) and Me_3PO (1.48 Å).[19] For such phosphine oxides multiple P−O bonding arises from overlap of an oxygen 2pπ orbital with phosphorus 3pπ or 3dπ orbitals or in more classical terms from contributions to the ground-state configuration from resonance forms **B** and **C**:

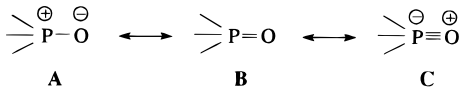

A **B** **C**

It could indeed be argued that clusters **3**$[H_2NPr^i_2]$ and **6**$[Et_4N]$ are trimetalated derivatives of phosphine oxide H_3PO although the angles subtended at the phosphorus atom by the three metal atoms (76.9−77.5° in **3**$[H_2NPr^i_2]$; 76.9−77.4° in **6**$[Et_4N]$) are significantly below the C−P−C angles found in the oxides.

The P−O bond length in **3**$[H_2NPr^i_2]$ is slightly longer (at the 3σ level) than that in **6**$[Et_4N]$, likely as a result of hydrogen bonding between the PO ligand oxygen atom and the hydrogen atoms on the ammonium cation [O(13)···H(1x) = 2.09 Å, O(13a)···H(1y) = 1.97 Å (a indicates the equivalent position $-x$, $1-y$, $1-z$)]. The ν(PO) frequencies in the $[H_2NPr^i_2]^+$ salts of **3** and **6** are at lower energies than those found in their $[Et_4N]^+$ counterparts (e.g. 1075 *versus* 1169 cm^{-1} for **3**; 1156 *versus* 1176 cm^{-1} for **6**) again as a result of differences in hydrogen bonding. Interestingly the ν(CO) frequencies in the anions are also influenced somewhat by hydrogen bonding with higher average ν(CO) values in the hydrogen-bonded $[H_2NPr^i_2]^+$ salts. Evidence that the PO ligand itself may have a π-acceptor capacity or alternatively is a poorer σ-donor than the phosphinidene ligand $PNPr^i_2$ is shown from the fact that the ν(CO) values in anionic **6**$[Et_4N]$ are only slightly lower than in the neutral cluster **5**.

The characterization of **3** and **6** brings to three the number of PO complexes described to date. However, a molecule isoelectronic with **3** and **6**, namely $[FeRu_3(CO)_{12}(NO)]^-$, has been reported by Gladfelter and Fjare.[20] This cluster contains a tetrahedral core of metal atoms similar to **3** and **6**, but the NO ligand is terminally bound to the iron atom. Another related

(18) (a) Band, E.; Muetterties, E. L. *Chem. Rev.* **1978**, *78*, 639. (b) Chi, Y.; Chuang, S.-H.; Liu, L.-K.; Wen, Y.-S. *Organometallics* **1991**, *10*, 2485.

(19) Goggin, P. L. in *Comprehensive Coordination Chemistry*; Wilkinson, G., Gillard, R. D., McCleverty, J. A., Eds.; Pergamon: Oxford, U.K., 1987; Vol. 2.

(20) Fjare, D. E.; Gladfelter, W. L. *J. Am. Chem. Soc.* **1984**, *106*, 4799.

Scheme 1

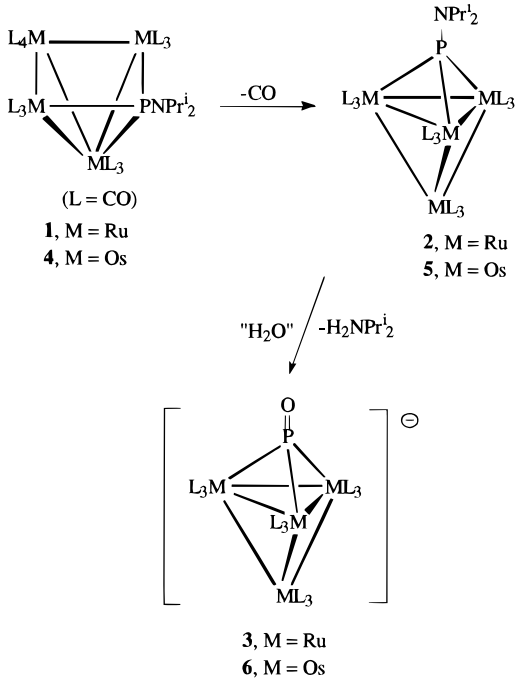

cluster which has not been structurally characterized is $Co_3(CO)_9(PS)$ in which a triply bridging PS ligand is postulated.[21]

The formation of **3** and **6** from **1** and **4** is shown in Scheme 1. The source of the elements of H_2O required to cleave the P−N bond of the diisopropyl phosphinidene group could be adventitious water in the solvent or basic and acidic sites on the surface of the silica gel. There is evidence that the latter may be the case since rigorously dried silica gel gave only traces of **3** and **6** from **2** and **5**. Moreover, **2** and **5** are stable in solvents containing small quantities of water with and without traces of acid or base.

(21) Vizi-Orosz, A.; Palyi, G.; Marko, L. *J. Organomet. Chem.* **1973**, *60*, C25.

Scheme 2

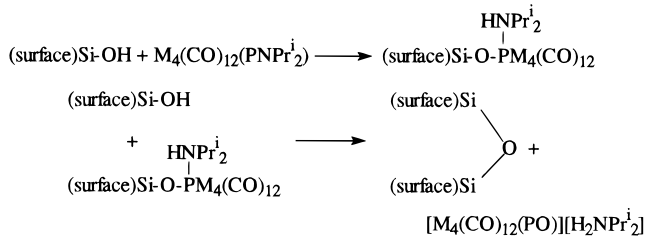

Recently[22] we have shown that P−N bond cleavage and P−O bond formation can be achieved in high yield via a sequence of protonation by strong acid followed by treatment with tetraalkylammonium hydroxide. Thus we can confidently propose the following mechanism for the formation of **3** and **6** on silica gel in which initial proton transfer from an acidic site or a silica surface to a lone pair of an isopropylamino substituent is followed by addition of an Si−OH group to the phosphinidene with loss of $[H_2NPr^i_2]^+$ and formation of a P−O bond (Scheme 2). This method of forming PO ligands via the hydrolysis of P−N bonds in readily accessible aminophosphinidene complexes would appear to offer greater scope for development than the oxidative cleavage of a P−P bond in diphosphorus-containing clusters.[6]

We are currently expanding the range of P═O complexes accessible via P−N bond scission reactions.

Acknowledgment. We thank the Natural Sciences and Engineering Research Council of Canada for financial support.

Supporting Information Available: Tables of complete fractional coordinates and isotropic thermal parameters, additional bond lengths and angles, and anisotropic thermal parameters for **1**, **2**, **3**$[H_2NPr^i_2]$, **4**, and **6**$[Et_4N]$ (32 pages). Ordering information is given on any current masthead page. Structure factor tables are available upon request from the authors.

OM960032O

(22) Wang, W.; Carty, A. J. unpublished results.